A practitioner's guide to fringe projection profilometry

Snehal Padhye, David Messinger, James A. Ferwerda; Rochester Institute of Technology; Rochester, New York

Abstract

Many techniques exist for 3D digitization of cultural heritage objects. Paintings, manuscripts, and other near-planar objects are especially challenging to digitize because of their minute surface variations. Of the existing techniques, fringe projection profilometry (FPP) is one of the most promising approaches for measuring the surface shape of such objects. In practical implementations of FPP, one needs to understand and control various sources of error due to system hardware and environmental conditions. It is difficult to find information on this in one place in the literature, which discourages application of the technique. In this paper we present a practitioner's guide to phase-shifting fringe projection profilometry that covers critical but often omitted implementation details required for successful application of the technique.

Introduction

3D digitization of cultural heritage objects usually involves capturing high resolution images of the objects from different viewpoints and/or under varying lighting conditions. Techniques like reflectance transformation imaging (RTI) [1] employ a fixed camera position and varying illumination to produce image-sets that can simulate surface relighting, but do not explicitly represent surface topography. Photogrammetric techniques [2] use images taken from multiple viewpoints to triangulate surface topography, but can be challenging to use when surfaces have low relief. Structured light (SL) [3] techniques can address both these limitations. SL works on the triangulation principal used in photogrammetry, but the patterns of light provide coded information about each pixel to find correspondences. Such techniques are limited by the resolution of the projector used to project the patterns because it needs to create a unique codeword for each pixel.

Fringe projection profilometry (FPP) [4] is a low-cost, high-precision, 3D digitization technique that uses structured light patterns to capture surface topography. In this technique, digital sinusoidal gratings are projected onto the object being digitized, and a digital camera captures images of the grating-illuminated object. Distortions and modulations of the gratings are then used to estimate 3D object properties. The surface measurement is based on phase retrieval and not on unique codewords at each pixel, making it independent of the projector resolution. While, in theory, the technique looks straightforward, there are many potential sources of error in practical implementations caused by the hardware components. In the following sections, we discuss the sources of these errors, and describe techniques to mitigate them to allow the effective use of FPP for digitization of cultural heritage objects.

Concept

The basic principle of FPP is to retrieve phase from sinewave gratings projected on the target surface as illustrated in Figure 1. The phase retrieval can be done in two ways. Fourier Transform Profilometry (FTP) [5] can calculate phase shift for the entire object using a single grating-projected image by retaining the modulated frequencies and filtering out others. It requires precise filtering of unwanted frequencies which can be unwieldy with real world data. In contrast, Phase-shifting FPP requires multiple grating-projected images but calculates the phase-shift at each pixel.
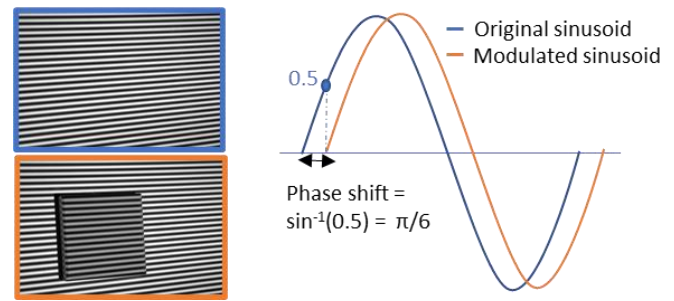

Figure 1 (Left) A sinusoidal grating and the sinusoid modulated by an object. (Right) An illustration of the phase shift caused by the object.

The minimum number of phase shifts required for applying phase shifting FPP is three. Using this minimum number makes the method fast and practical for real-time application. Here, three sine gratings with relative phases of 0, $2\pi/3$ and $4\pi/3$ radians are projected onto a target and the modulated phases are calculated from the captured images using the following equations:

$$i_n = a + b\,cos(2\pi f x - 2\pi n/N) \qquad (1)$$

$$I_n = A + B\,cos(\varphi - 2\pi n/N) \qquad (2)$$

where i_n are the projected sine gratings, I_n are the captured images with n = 0, 1, 2, a = b = 0.5 and N = 3. Φ, A and B are calculated as:

$$\varphi = tan^{-1}\frac{\sqrt{3}\,(I_1 - I_2)}{2I_0 - I_1 - I_2} \qquad (3)$$

$$A = \frac{I_0 + I_1 + I_2}{3} \qquad (4)$$

$$B = \frac{1}{3}\sqrt{(3(I_1 - I_2)^2 + (2I_0 - I_1 - I_2)^2)} \qquad (5)$$

'A' is the average intensity, 'B' is the intensity modulation and φ is the desired phase. 'a' and 'b' are each given a value of 0.5 to cover the entire dynamic range of the projector [6]. The phase (φ) has the principal values of the arctan function in the range [-π, π], and we need to "unwrap" the values to obtain a continuous measure of the phase. Phase unwrapping is performed by adding 2πk (where k is an integer) at every discontinuity at each -π and π. Many standard libraries provide APIs to do phase unwrapping [7][8]. An unwrapped phase can first be calculated for a reference plane and then we can obtain a depth map for the target object by subtracting the object's phase map from that of the reference plane. The depth map obtained in terms of phase values (in radians) can be converted to world coordinates by different approaches discussed later in this paper. The entire pipeline is depicted in Figure 2.

Implementation Details

FPP can be implemented by using a DSLR and a digital Projector mounted side by side as shown in Figure 3. Here, we are using a Canon XSi DSLR with an 18-55 mm zoom lens and an LG HF60LA DLP projector. The quality of FPP depth estimates depends highly on the gratings being perfectly sinusoidal, so it is important to know whether our capture and display systems preserve these sinusoidal properties. If not, we must first correct them through system calibration.

Camera characterization can be performed by capturing an image of a ColorChecker chart and plotting the relationship between input and output gray scale values. A colorimeter can be used to measure the output of a projector, and a similar relationship of input and output gray scale values can be established. Both the camera and the projector have non-linear responses and need to be linearized. Incoming pixel values are multiplied with the inverse of the device non-linear response to ensure the projected and captured patterns are linear with respect to the digital sinusoidal input values. If a ColorChecker chart and colorimeter are not available for the individual device characterization, we can consider the input – output relationships of the system as a whole. A range of grayscale values can be projected and captured, and the relationship between input and output intensities can be observed as shown in Figure 4. Individual non-linearities often approximately compensate each other to give a quasi-linear system response, and one can choose intensities in the linear range to represent the input sinusoid. An inverse function of this system response can also be used with the incoming sinusoids to ensure linearity.

Sampling and quantization limits in the digital devices can also cause the projected and captured grating patterns to deviate from ideal sinusoids which can introduce additional errors. The projector has a fixed resolution, and the number of pixels per cycle decreases for increasing sinusoidal frequency as shown in Figure 5. The camera has similar limitations on the capture end. Therefore, it is important, to choose the grating frequency such that the displayed/captured grating images are not distorted. The range of projected grayscale values should be such that it does not cause clipping in the displayed images. The camera exposure should also be set such that the captured images are not saturated. If the system settings are not optimal, it may lead to quantization errors as shown in Figure 6. In addition, the camera aperture should be as small as
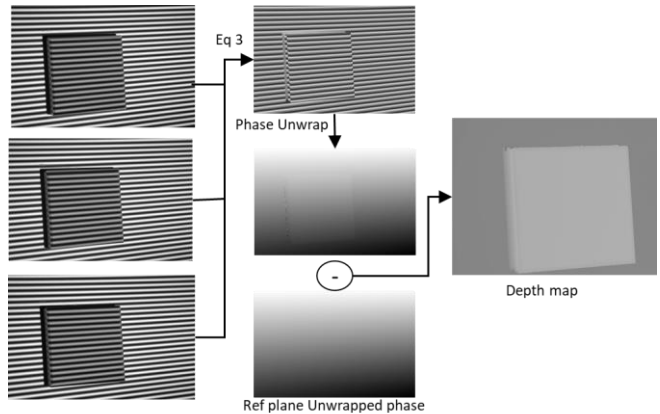

Figure 2 Three-phase FPP: Three phase-shifted gratings are projected on a target object and images are captured. Equation 3 is used to calculate wrapped phase shifts, and phase unwrapping is performed to get continuous phase shifts. The unwrapped phase subtracted from that of a reference plane gives a depth map of the object.

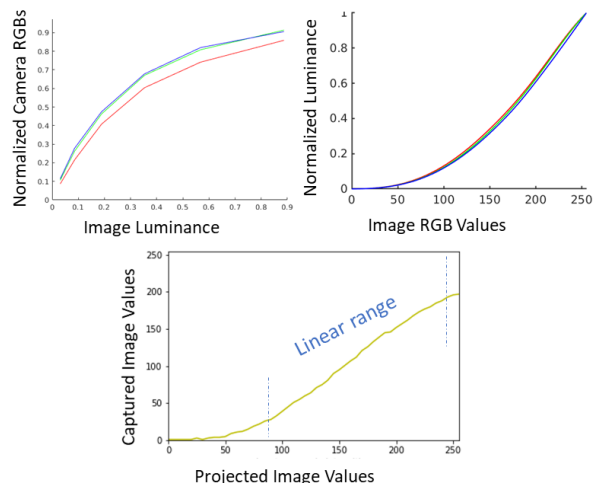
Figure 3 A typical projector-camera rig for FPP.

Figure 4 (Top Left): Camera non-linear response. (Top Right): Projector non-linear response. (Bottom): Camera-projector combined system response.
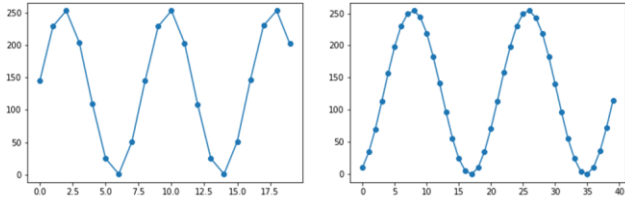
Figure 5 *Sampling errors in FPP (Left): Sinusoid constructed with 8 pixels per cycle shows shape errors due to the low sampling rate. (Right): Sinusoid constructed with 18 pixels per cycle more closely approximates the ideal shape and creates a smoother sinusoid. Projector resolution is [1920,1080].*
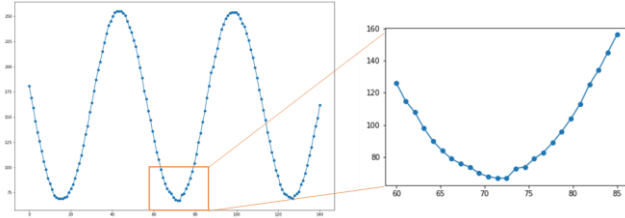

Figure 6 *Quantization errors in FPP (Left): Captured sinusoid. (Right): Zoomed trough of the sinusoid showing quantization errors.*

Figures 9 and 10 show some additional examples of the technique in action.
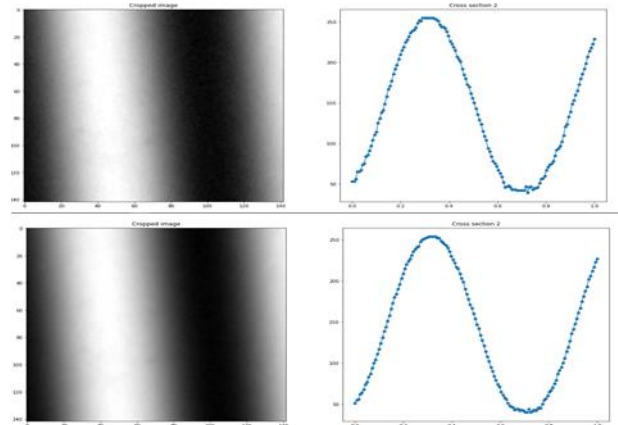

Figure 7 *Reducing intensity noise errors (Top) Cross section of the captured sinusoid of a single frame. (Bottom) Cross section of the captured sinusoid averaged over 5 frames.*
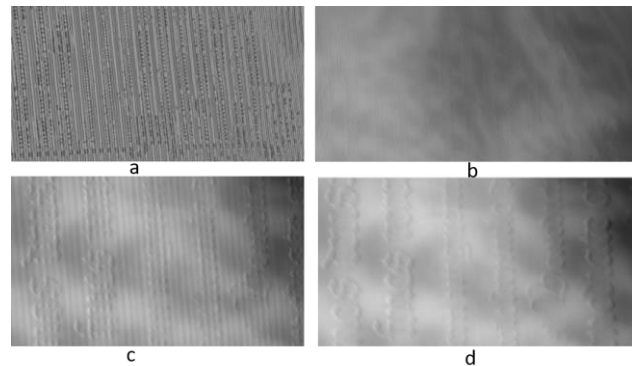

Figure 8 *Reducing harmonic errors.* ***a*** *Depth map of a manuscript by phase shifted FPP,* ***b.*** *depth map after removing random noise,* ***c.*** *zoomed in version to show harmonic error and* ***d.*** *depth map of the manuscript after double shift FPP.*
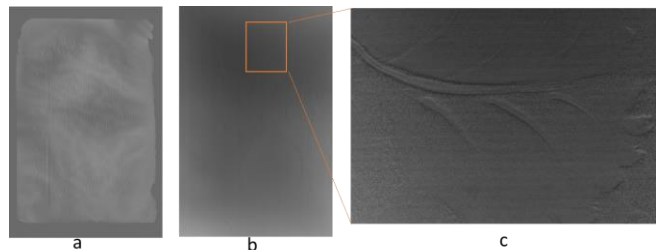

Figure 9 *Surface variations shown by* ***a*** *depth map of an entire manuscript,* ***b.*** *depth map of a painting,* ***c.*** *zoomed in version of the painting that shows paint strokes of a leaf.*
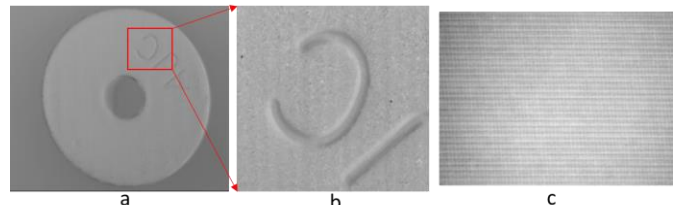

Figure 10 *Depth maps of small objects with different material properties* ***a*** *Depth map of a 1.25mm thick metallic washer,* ***b.*** *zoomed version of the washer showing the depth of letter inscribed on the washer,* ***c.*** *Mesh of a canvas board captured through FPP.*

possible to provide larger depth of field and both the projector and camera should be focused to display and capture sharp gratings.

Once the setup is done and sinusoids are generated, the grating images are projected one by one onto the target object and the illuminated object is captured by the camera. In our system, we use the Gphoto2 [9] and Python OpenCV [10] libraries to control projection and capture. Once the images are captured, they are processed to get unwrapped phase. Here, we use the 'unwrap_phase' API from the Scikit-Learn [8] library which is based on [11] for phase unwrapping.

Even with optimal setup, there can still be in error in the system due to intensity noise, non-linearities, and illumination fluctuation, and we need methods to overcome each one of them. As a first step, we can reduce intensity noise by taking multiple images and averaging them. Figure 7 shows a cross section of single vs averaged sinusoid images. This step itself can reduce the errors as shown in Figure 8. A depth map of a manuscript produced by three-phase FPP using single image is shown in Figure 8a, and the result of applying FPP after taking the average of 5 images is shown in Figure 8b.

Another source of error can be seen in the Figure 8c, where non-linearities still present in the projector and camera transfer functions produce depth maps corrupted by sinusoidal harmonics. While linearizing the system response reduces this error, it is difficult to perform perfect linearization, and residual errors in both projection and capture devices lead to errors in depth estimates. Baker et al. [12] showed that a phase error occurs due to these residual nonlinearities in the system, and that the period of this harmonic error is proportional to the number of phase shifts of the captured gratings. For three-phase FPP, the error will have third order harmonics of the projected grating frequency (higher frequency patterns seen in Figure 8c). To overcome this error, we can project a second set of fringe patterns with a relative phase difference of 60 degrees. This makes the phase differences between the harmonics in the two fringe sets 3 x 60 = 180 degrees. Averaging the phase shifts obtained from these two sets of images, cancels the contributions of the harmonics. This method is known as double-shift three-phase FPP [13], and its result is shown in Figure 8d.

The third source of error, illumination fluctuation, is typically not a problem with modern digital projectors having LED light sources. To confirm this, we measured the luminance of our projector at five-minute intervals and observed that its output is essentially constant over time as shown in Table 1. The luminance of the projector appears to have very small variations of 0.8% and does not require it to be kept on for some time to reach equilibrium.

In addition to the sources of luminance error outlined above, the depth estimation is also sensitive to the orientation of the projected gratings. The gratings should be oriented such that the direction of phase shift is parallel to the baseline of the camera and projector as shown in Figure 11. Figure 12 shows differences in the depth maps obtained when the phase shift direction is parallel (a) and perpendicular (b) to the system baseline. It can be difficult to achieve this when working with real devices. In such cases, the errors can be minimized by adjusting the orientation of the fringes mathematically as discussed in [14].

Reading	Y
1	13659
2	13277
3	13501
4	13499
5	13376
6	13294
7	13546
8	13444
9	13373
10	13373
11	13336

Table 1 *Projector luminance measured at 5 minutes interval using colorimeter shows very small variation in luminance.*

The presence of highly specular materials can also cause an incorrect jump in measured values in FPP. This problem can be eliminated by installing crossed polarizers on the projector and camera which effectively cancels specular reflections. Figure 9 showed a depth map of a metallic object obtained by reducing specular components using cross-polarization.

The conversion of the phase map (in radians) to height (in mm) can be done in various ways. One common approach is to perform geometric calibration of the projector-camera system and convert the angular depth map values to heights by applying a transformation using intrinsic and extrinsic matrices of the projector/camera system [15]. Another approach is to calculate a scaling factor by using the ratio of height of a known object to its calculated depth in radians. A constant scaling factor for an entire image or a per-pixel scaling factor can be used to do this conversion. A linear scaling factor may not work for all range of objects and we might need to perform non-linear scaling as discussed in [16]. However, in the constraint of near-planar objects like manuscripts and paintings, where the depth variation is very small, the linear relationship appears to work sufficiently well [16]. Apart from this, the phase to height relationship can also be derived by applying least squares estimation [17] from measurements of some of the known calibration objects [18]. A reference plane can be moved in small increments and a look-up table [19] can be constructed between the observed phase value and known height value and used for mapping.

In our system we have used the constant scaling method, and 3D representations of some objects are shown in Figure 13.
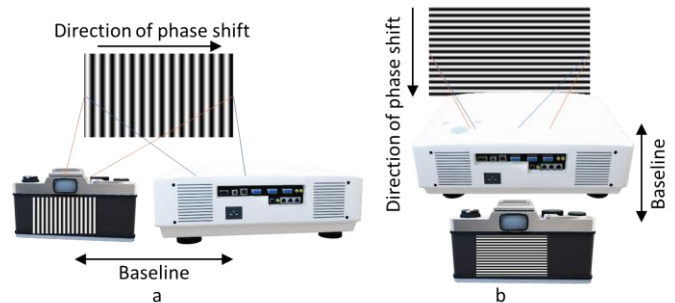

Figure 11 *Orientation of the gratings should be such that the direction of phase shift is parallel to the baseline of the system. **a** and **b** show examples of two configurations of the system and the ideal orientations of the gratings in the respective arrangements.*
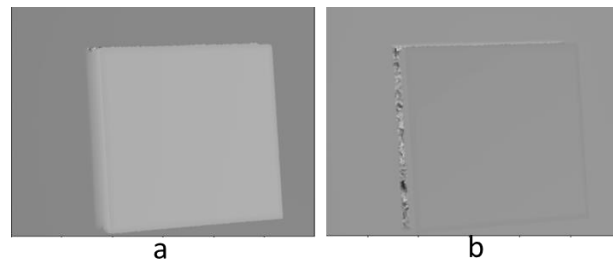

Figure 12a *Depth map of a cube with projected fringe phase shift direction parallel to the system baseline. **b** Depth map of the same cube with projected fringe direction perpendicular to system baseline.*
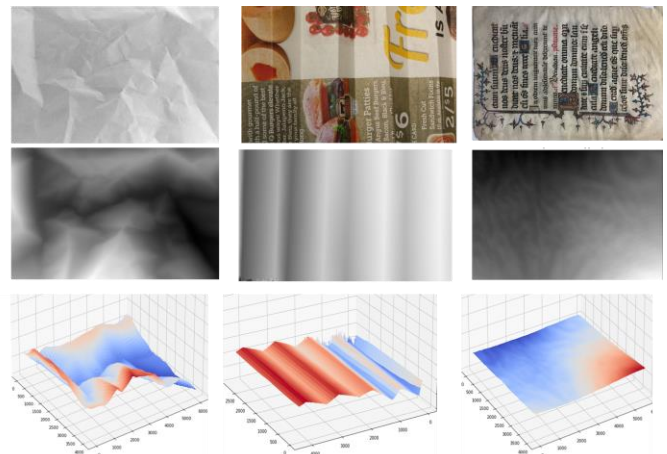

Figure 13 *Each column shows an image of the object, its depth map, and its 3D representation. First column consists of a crumpled paper, second column consist of newspaper shaped as a triangular grating and the third column represents a manuscript from Cary collections at RIT.*

Conclusion

Fringe projection profilometry is a low-cost, high precision, 3D capture technique that has great potential to facilitate the digitization of cultural heritage objects. In this paper we have outlined common sources of error in the depth estimates produced by the technique and have described methods for eliminating or minimizing these errors. We hope that these practical methods will facilitate the wider use of FPP in the cultural heritage imaging community.

Acknowledgement

We thank the Cary collection at RIT for allowing us to use one of their manuscripts to demonstrate our results.

References

[1] Reflectance Transformation Imaging, http://culturalheritageimaging.org/Technologies/RTI/

[2] Photogrammetry, http://culturalheritageimaging.org/Technologies/Photogrammetry/

[3] Y. Francken, T. Cuypers, T. Mertens, J. Gielis and P. Bekaert, "High quality mesostructure acquisition using specularities," IEEE Conference on Computer Vision and Pattern Recognition, pp. 1-7 (2008).

[4] V. Srinivasan, H. Liu, and M. Halioua, "Automated phase-measuring profilometry of 3-D diffuse objects," Appl. Opt. 23, 3105-3108 (1984).

[5] X. Su and W. Chen, "Fourier transform profilometry: a review," Optics and Lasers in Engineering, Volume 35, Issue 5, Pages 263-284 (2001).

[6] C. Zuo, S. Feng, L. Huang, T. Tao, W. Yin, Q. Chen," Phase shifting algorithms for fringe projection profilometry: A review", Optics and Lasers in Engineering, Volume 109 (2018).

[7] Numpy unwrap phase API, https://numpy.org/doc/stable/reference/generated/numpy.unwrap.html.

[8] Scikit-learn unwrap phase API, https://scikit-image.org/docs/dev/auto_examples/filters/plot_phase_unwrap.html.

[9] Gphoto2 Library - https://pypi.org/project/gphoto2/.

[10] Python-OpenCV - https://pypi.org/project/opencv-python/.

[11] M.A. Herraez, D.R. Burton, M.J. Lalor, and M.A. Gdeisat, "Fast two-dimensional phase-unwrapping algorithm based on sorting by reliability following a noncontinuous path", Journal Applied Optics, Vol. 41, No. 35, pp. 7437 (2002).

[12] M.J. Baker, J. Xi and J.F. Chicharo, "Elimination of Non-linear Luminance Effects for Digital Video Projection Phase Measuring Profilometers," 4th IEEE International Symposium on Electronic Design, Test and Applications (delta 2008), Hong Kong, China (2008).

[13] P. Huang, Q. Hu, and F. Chiang, "Double three-step phase-shifting algorithm," Appl. Opt. 41, 4503-4509 (2002).

[14] Yajun Wang and Song Zhang, "Optimal fringe angle selection for digital fringe projection technique," Appl. Opt. 52, 7094-7098 (2013).

[15] Z. Huang, J. Xi, Y. Yu, Q. Guo, and L. Song, "Improved geometrical model of fringe projection profilometry," Opt. Express 22, 32220-32232 (2014).

[16] P. Jia, J. Kofman, C.E. English, "Comparison of linear and nonlinear calibration methods for phase-measuring profilometry," Opt. Eng. 46(4) 043601 (2007).

[17] L. Huang, P.S.K. Chua, and A. Asundi, "Least-squares calibration method for fringe projection profilometry considering camera lens distortion," Appl. Opt. 49, 1539-1548 (2010).

[18] M. Vo, Z. Wang, T. Hoang, and D. Nguyen, "Flexible calibration technique for fringe-projection-based three-dimensional imaging," Opt. Lett. 35, 3192-3194 (2010).

[19] M. Fujigaki, T. Sakaguchi, Y. Murata, "Development of a compact 3D shape measurement unit using the light-source-stepping method," Optics and Lasers in Engineering, Volume 85, (2016).

Author Biography

Snehal A. Padhye is a third year PhD. student in the Chester F. Carlson Center for Imaging Science at RIT. She received a BS in Electronics and MS in Signal Processing from India. Her dissertation research work focuses on designing hardware and software systems for capturing and visualizing realistic digital models of cultural heritage objects.

David Messinger is a professor in the Chester F. Carlson Center for Imaging Science at RIT. He received a BS in Physics from Clarkson University and Ph.D. in Physics from Rensselaer Polytechnic Institute. His research interests include developing methods to extract quantitative information from spectral imagery and the use of remote sensing techniques for multi-disciplinary research.

James A. Ferwerda is an Associate Professor in the Chester F. Carlson Center for Imaging Science at RIT. He received a B.A. in Psychology, M.S. in Computer Graphics, and a Ph.D. in Experimental Psychology, all from Cornell University. The focus of his research is on building computational models of human vision from psychophysical experiments and developing advanced imaging systems based on these models.